

# Downhill Protein Folding Modules as Scaffolds for Broad-Range Ultrafast Biosensors

Michele Cerminara,<sup>†</sup> Tanay M. Desai,<sup>†,‡</sup> Mourad Sadqi,<sup>†</sup> and Victor Muñoz<sup>\*,†,‡</sup>

<sup>†</sup>Centro de Investigaciones Biológicas, Consejo Superior de Investigaciones Científicas (CSIC), Ramiro de Maeztu 9, Madrid 28040, Spain.

<sup>‡</sup>Department of Chemistry & Biochemistry, University of Maryland, College Park, Maryland 20742, United States

**S** Supporting Information

**ABSTRACT:** Conformational switches are macromolecules that toggle between two states (active/inactive or folded/unfolded) upon specific binding to a target molecule. These molecular devices provide an excellent scaffold for developing real-time biosensors. Here we take this concept one step beyond to build high-performance conformational rheostat sensors. The rationale is to develop sensors with expanded dynamic range and faster response time by coupling a given signal to the continuous (rather than binary) unfolding process of one-state downhill folding protein modules. As proof of concept we investigate the pH and ionic-strength sensing capabilities of the small  $\alpha$ -helical protein BBL. Our results reveal that such a pH/ionic-strength sensor exhibits a linear response over 4 orders of magnitude in analyte concentration, compared to the 2 orders of magnitude for switches, and nearly concentration-independent microsecond response times.

The development of biosensors has become a thriving research area.<sup>1–3</sup> In general, building efficient biosensors involves two steps: specific binding to the analyte and a readout signal. Proteins and nucleic acids are attractive biosensor scaffolds because they can bind vast collections of markers with extremely high affinity (down to pM) and amazing specificity.<sup>1,4</sup> Turning biomolecules into sensors requires coupling a conformational change to the binding event.<sup>5</sup> One possibility is to employ proteins that switch naturally between conformations upon binding.<sup>6</sup> A more general approach relies on engineering the macromolecule's stability and/or structure to trigger complete folding (or unfolding) upon binding to the analyte. The latter has been successfully implemented for nucleic acids (molecular beacons)<sup>7</sup> and protein-based sensors that use either folding coupled to binding<sup>8</sup> or alternate frame folding.<sup>9</sup> Developing protein sensors is more challenging, but, in turn, protein sensors offer a broader spectrum of potential binding partners.<sup>5</sup> Another potential advantage of conformational switches is their promise of affording real-time detection.<sup>10</sup>

There are, however, intrinsic limitations for using conformational switches as biosensors. A most critical one is their narrow dynamic range. Because the signal emerges from the cooperative conversion between the off- and on-states, the sensor only detects differences in concentration within 10-fold

above or below the analyte dissociation constant ( $K_d$ ).<sup>11</sup> Strategies to match the  $K_d$  to the desired concentration are thus essential, e.g., by fine-tuning the macromolecule's stability.<sup>11,12</sup> However, in the end, broad-range sensitivity is only achieved by arranging multiple switches in tandem.<sup>13</sup> Moreover, the complex (potentially slow) kinetics of folding coupled to ligand binding might hamper the application of molecular switches as fast sensors.

In this regard, the discovery of downhill folding<sup>14–16</sup> offers exciting opportunities for developing improved biosensors. Downhill folding proteins fold in microseconds, without crossing significant free energy barriers.<sup>16,17</sup> In the extreme case there is no free energy barrier at all, and thus the protein populates a single conformational ensemble that becomes progressively disordered as a function of denaturational stress (one-state downhill).<sup>18</sup> Such gradual one-state unfolding could be accompanied by proportionate changes in ligand affinity, similarly to the fly-casting mechanism,<sup>19</sup> effectively turning the downhill folding module onto a conformational rheostat<sup>20</sup> (Figure 1). Theoretically, these molecular rheostats could

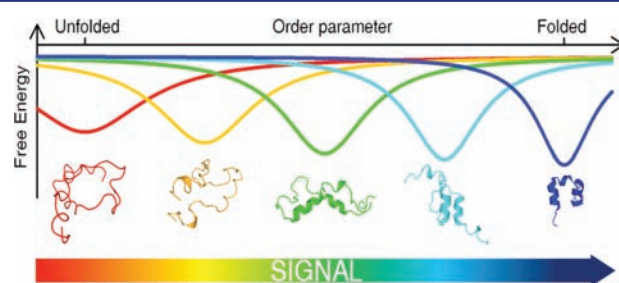


**Figure 1.** Sketch of a molecular rheostat based on the coupling of a signal (e.g., proton binding) to the folding ensemble of a one-state downhill folding protein module.

provide expanded dynamic range toward the analyte. Moreover, due to their microsecond folding times, downhill modules could make for much faster biosensors.

Here we explore the molecular rheostat concept aiming at developing a proof of principle for broad-range ultrafast biosensing. We chose the small  $\alpha$ -helical protein BBL for this initiative. BBL folds/unfolds in microseconds<sup>21</sup> and has a weakly cooperative unfolding process.<sup>15</sup> The one-state downhill

Received: February 2, 2012

Published: May 3, 2012

folding mechanism of BBL has been observed with many approaches, including atomic resolution equilibrium unfolding experiments,<sup>22</sup> differential scanning calorimetry,<sup>23</sup> multiprobe laser T-jump kinetics,<sup>21</sup> single-molecule fluorescence spectroscopy,<sup>24</sup> and large-scale molecular dynamics simulations.<sup>25</sup>

BBL readily unfolds in the pH 7–3 range, refolding back to its native 3D structure upon increasing the ionic strength.<sup>26</sup> This behavior provides the molecular basis for pH and ionic-strength sensing. The BBL 3D structure points to two buried histidines (H13 and H37), which are involved in several tertiary interactions that bring the two helices together, as major players (Figure 2). A pH titration using NMR rendered  $pK_a$  values of

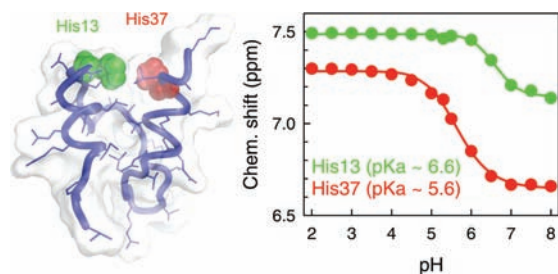


**Figure 2.** Two buried histidines in BBL as the basis for pH and ionic-strength sensing. Left: 3D structure of BBL, with the two buried histidines highlighted. Right: their pH titration monitored by the changes in amide proton chemical shift.

$\sim 5.6$  and  $\sim 6.6$  for H37 and H13, respectively (Figure 2). The  $pK_a$  of H13 is similar to that of free histidine. For H37 the  $pK_a$  is 1 pH unit lower, indicating that the native structure strongly favors the nonprotonated form. In addition, BBL has five negatively charged residues (three E and two D) that could also contribute to unfolding at the more acidic conditions. Overall, these results suggest that the partial unfolding of BBL at moderately low pH is largely controlled by the ionization of H37.

To monitor the conformational behavior of BBL, we used far-UV circular dichroism (CD), which mainly reports on its  $\alpha$ -helix content. We investigated the role of pH by performing CD equilibrium thermal unfolding experiments at different pH values. These experiments revealed two effects associated with lowering pH: a decrease in midpoint denaturation temperature ( $T_m$ ), and a reduction of native CD signal in the pre-transition baseline (Figure S1). Interestingly, the two effects combined produce a monotonic change in CD over an extraordinarily broad pH range. Under conditions of thermal stability (i.e., 273–298 K<sup>27</sup>) the BBL CD signal decreases linearly between pH 8 and 3.5 (Figure 3A and Figure S2). Below pH 3.5 the change becomes more abrupt, probably due to the concerted titration of the five acidic residues. Therefore, the conformational ensemble of BBL responds in linear fashion to differences of  $>4$  orders of magnitude in  $H^+$  concentration. This dynamic range is greatly expanded relative to a conformational switch with an apparent  $pK_a = 5.6$ , which would produce a sigmoidal CD curve with a width of 2 pH units (Figure 3A). The signal at 222 nm reports on a change of the entire BBL CD spectrum. The modified spectrum indicates a large conformational change that is consistent with the transformation of the native BBL  $\alpha$ -helix structure into random coil conformations (Figure 3B). Singular value decomposition (SVD) of the spectra as a function of pH confirms this interpretation (inset to Figure 3B). The second SVD component does show a typical random

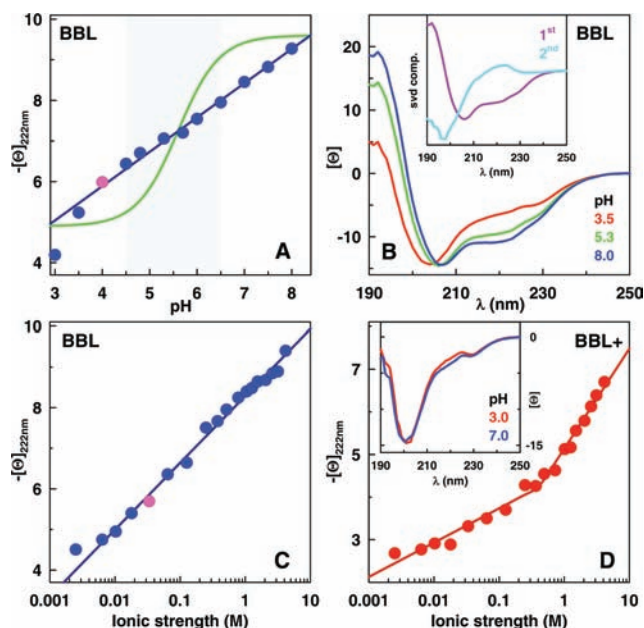


**Figure 3.** Measuring pH or ionic strength from the CD signal of BBL variants at 273 K. Panels A, C, and D show the negative molar ellipticity at 222 nm. Panel B and inset to panel D show true molar ellipticities. (A) Effect of pH on BBL (blue). The green curve is a calculation of the behavior expected for a conformational switch with  $pK_a = 5.6$ . The gray swath covers the dynamic range of the switch. (B) Far-UV CD spectrum of BBL at various pH values. The first two SVD components are shown in the inset. (C) Effect of ionic strength on BBL at pH 4 using LiCl as salt. The magenta circles in A and C signal the matching conditions. (D) Effects of pH (inset) and ionic strength (main) on a BBL variant with the three E and two D replaced with Q and N, respectively (BBL+). The ionic-strength dependence was measured at pH 4 for comparison with panel C.

coil CD spectrum that grows in amplitude as pH decreases. These results highlight the coupling between proton binding and BBL unfolding, and demonstrate the capacity of BBL to operate as an extremely broad-range pH sensor.

In principle, BBL might also be able to sense ionic strength given that electrostatic interactions modulate its unfolding. An increase in ionic strength should thus refold protonated BBL by electrostatic shielding. This functionality is shown in Figure 3C. Upon increasing the ionic strength at pH 4, the CD signal of BBL becomes more native-like, eventually reaching the values of high pH (Figures 3C and S3). Moreover, there is direct correspondence between the measured signals along the pH and ionic-strength dependencies (e.g., magenta circles in Figure 3A,C). The effect is independent of the type of salt and buffer employed,<sup>26</sup> consistent with electrostatic screening rather than specific ion binding. Therefore, Figure 3C indicates that protonated BBL responds continuously to changes in ionic strength spanning at least 3 orders of magnitude. These experiments demonstrate that BBL can also operate as a broad-range ionic-strength sensor.

The sensitivity of BBL to both pH and ionic strength brings about the issue of crosstalk between the two properties. To address this issue we designed and synthesized a BBL variant that eliminates the five negative charges of wild-type BBL by replacing E with Q and D with N. This variant, which we term BBL+, is positively charged over the pH 2–12 range. CD experiments showed that BBL+ is completely unfolded, regardless of pH (inset to Figure 3D). In fact, BBL+ is as

unfolded as BBL is at pH 2. However, BBL+ is sensitive to ionic strength and partly refolds as its positive charges become screened with salt (Figures 3D and S4). The response to ionic strength of BBL+ is slightly more complex (i.e., bilinear), but it covers the same dynamic range as shown in Figure 3C. Therefore, combining BBL and BBL+ allows for a straightforward control of the crosstalk and thus for simultaneous monitoring of pH and ionic strength.

Another factor for defining biosensor performance is the response time, which is particularly relevant for real-time detection.<sup>10</sup> Devices based on folding coupled to binding have response times determined by the kinetic interplay between folding and complex formation. To investigate this interplay we built a kinetic model for two-state folding coupled to binding (SI). Simulations with the model reveal that the time response of conformational switches is characterized by two extreme regimes. At very low ligand concentration the kinetics is limited by the complex dissociation rate constant ( $k_{\text{off}}$ ). When ligand concentration is high enough to approach binding saturation, kinetics becomes limited by the folding rate constant ( $k_{\text{F}}$ ). This implies that the overall rate shifts from one regime to the other over the dynamic range of the sensor (from 0.01 to 0.99 binding saturation). Practically, the response time is determined by the slowest regime. For a pH switch with  $\text{p}K_{\text{a}} = 5.6$  and binding controlled by proton transfer rates of  $\sim 5 \times 10^{10} \text{ M}^{-1} \text{ s}^{-1}$ ,<sup>28</sup> the limiting factor becomes the protein folding kinetics. Using an empirical estimate of  $1 \text{ s}^{-1}$  for the average  $k_{\text{F}}$  of switches based on two-state folding domains (see SI), such a pH sensor will exhibit kinetics of  $1/(10 \text{ ms})$  at high pH, but it will decrease to  $1/(1 \text{ s})$  at acidic pH (Figure S5). The overall response time would thus be  $\sim 1 \text{ s}$ . Switches that bind to complex molecules with high affinity will be further limited by the extremely small  $k_{\text{off}}$ . For example, a sensor with an apparent  $K_{\text{d}} = 10 \text{ nM}$  (ligand concentration that results in 50% binding), a folding equilibrium constant of  $10^{-3}$ , and diffusion-controlled association ( $\sim 10^8 \text{ M}^{-1} \text{ s}^{-1}$ ) will have an estimated response time in the order of 15 min (SI).

To check the response time of biosensors experimentally one can employ kinetic methods that measure the conformational relaxation of the macromolecule after perturbing the folding/binding coupled equilibria. We thus investigated the response time of our sensor by measuring the BBL folding/unfolding relaxation kinetics at various pH and ionic-strength values using the nanosecond laser-induced temperature-jump method. The partial unfolding induced by the T-jump on BBL favors an increase in protonation, resulting in coupled folding/binding kinetics. To follow the BBL folding/unfolding relaxation we employed infrared detection, which monitors the same conformational change observed by CD. The left panel of Figure 4 shows the kinetic decays measured for BBL at a final temperature of  $\sim 310 \text{ K}$  (i.e., physiological temperature) and pH values corresponding to H37 protonation fractions of  $\sim 0.97$ ,  $0.67$ , and  $0.04$ . The BBL relaxation rate as function of temperature is shown in Figure S6. The effects of ionic strength are shown on the right panel of Figure 4.

The laser T-jump experiments reveal that BBL folds/unfolds in a few microseconds at all conditions. The protein exhibits decays that are always well fitted to single exponential functions (black lines). These results indicate that the BBL pH/ionic-strength sensor can achieve a time resolution of  $10 \mu\text{s}$ , that is, many orders of magnitude faster than an equivalent conformational switch (Figure S5). Another interesting observation is that the relaxation time changes very little with pH and ionic

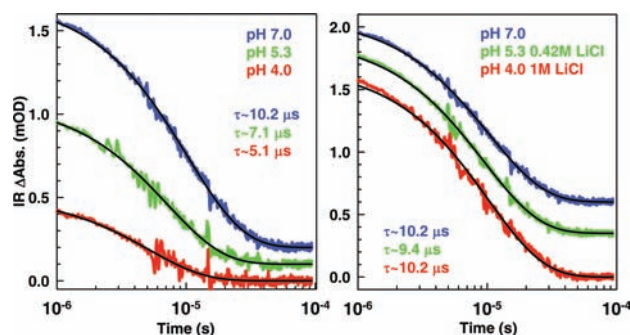


**Figure 4.** Time response of BBL as pH/ionic-strength sensor. The conformational relaxation kinetics of BBL at different pH and/or LiCl concentrations measured by infrared after  $\sim 10 \text{ K}$  laser-induced T-jumps to a final temperature of  $310 \text{ K}$ . Blue and green traces are shifted on the ordinate for clarity.

strength. A 1000-fold increase in  $[\text{H}^+]$  accelerates the relaxation by a mere 2-fold (pH 4 vs 7; Figure 4 left). Likewise, increasing ionic strength at a given pH has minimal effects on the BBL conformational dynamics (e.g., pH 4 and 5.3 in Figure 4). In fact, the ionic strength just counteracts the mild acceleration induced by partial protonation. The pH/ionic-strength compensation is apparent in the right panel of Figure 4, which shows decays for various pH values with amounts of LiCl matched to exactly compensate the pH-induced destabilization (i.e., the ionic strength that brings the BBL CD signal to that observed at neutral pH, see Figure S3). The almost identical decay amplitudes further confirm the matching conditions. Therefore, the kinetics of proton binding and release as well as the electrostatic screening by ionic strength affect minimally the microsecond conformational dynamics of BBL. Relaxation kinetics that is nearly independent of analyte concentration is a highly desirable property for biosensors because it enormously facilitates the optimization of response times.

We have shown that the downhill folding protein BBL can function as a pH and ionic-strength biosensor featuring unprecedentedly broad dynamic range and nearly concentration-independent ultrafast response times. As practical demonstration we employed the BBL system to monitor the change in pH occurring by the transformation of  $\text{CO}_2$  into carbonic acid upon dissolution in water. In this experiment a sudden infusion of  $\text{CO}_2$  drops the pH of the BBL solution to a value that depends on  $\text{CO}_2$  solubility and the presence of a buffer at a given concentration (SI). The BBL sensor effectively monitors the changes in pH over the entire experimental range (8–4.8) in real-time, reaching the values expected from the calibration (Figure 5). This experiment exploits the broad dynamic range of BBL and demonstrates that increasing buffer concentration in the mM range (resulting in proportionally higher final pH) slows down the kinetics from a few seconds to several minutes.

Therefore, our results provide a proof of concept for biosensors based on conformational rheostats. Furthermore, the experiments on BBL demonstrate that such devices can offer far superior performance than conformational switches. However, this work represents the very first step. At this point the application of conformational rheostats is limited to sensing pH and ionic strength, which involve multiple proton binding sites. Simulations with a one-dimensional free energy surface model of protein folding<sup>29</sup> reveals that reproducing the ultrabroad pH dynamic range of BBL requires a one-state

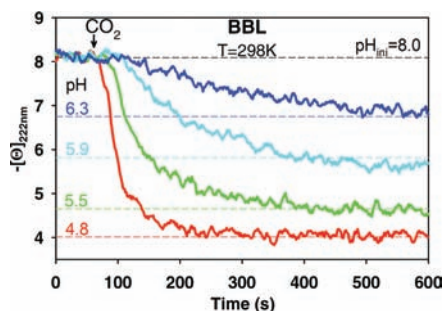


**Figure 5.** Real-time monitoring of pH changes induced by CO<sub>2</sub> dissolution. Experiments started at pH 8 with different buffer concentrations. The final pH reading is shown on the left column. The time of CO<sub>2</sub> infusion is shown with an arrow. Dashed lines show the CD signal expected from the BBL calibration given the final pH and ionic strength for each experiment.

downhill module, multiple proton binding sites (at least three sites with different  $pK_a$ : H13, H37, and one acidic residue), and gradually changing affinities as a function of unfolding (Figures S7 and S8). However, one-state folding is definitely an essential feature. This is easily shown on simulations performed with the same set of three proton binding sites with gradual affinity implemented on a two-state folding protein (Figures S7 and S8).

Developing novel conformational rheostat sensors is thus an exciting avenue for future research. Bearing it to full fruit will require further developments. One of them is the implementation of accurate theoretical-computational methods for identifying molecular rheostat candidates (i.e., downhill modules that bind specific molecular targets in a gradual fashion). It would also be useful to develop tools for engineering downhill folding modules via sequence design and manipulation. Such tools are required to efficiently turn downhill modules into rheostat sensors and tune their stability. Finally, efficient strategies for the implementation of high-sensitivity readouts that change continuously with unfolding (e.g., FRET) are critical for implementing rheostat sensors that work at the single-molecule level. The latter is an important nanobiotechnological goal since such devices would allow fast monitoring of changes in analyte concentration inside living cells with nanoscale resolutions.

## ■ ASSOCIATED CONTENT

### 📄 Supporting Information

Additional experiments, theoretical calculations and models, and experimental procedures. This material is available free of charge via the Internet at <http://pubs.acs.org>.

## ■ AUTHOR INFORMATION

### Corresponding Author

vmunoz@cib.csic.es

### Notes

The authors declare no competing financial interest.

## ■ ACKNOWLEDGMENTS

This work was supported by the Marie Curie Excellence Grant MEXT-CT-2006-042334, and grants BFU2008-03237 and CONSOLIDER CSD2009-00088 from the Spanish Ministry of Science and Innovation.

## ■ REFERENCES

- (1) Hellinga, H. W.; Marvin, J. S. *Trends Biotechnol.* **1998**, *16*, 183.
- (2) Castillo, J.; Gaspar, S.; Leth, S.; Niculescu, M.; Mortari, A.; Bontidean, L.; Soukharev, V.; Dorneanu, S. A.; Ryabov, A. D.; Csoregi, E. *Sens. Actuators B-Chem.* **2004**, *102*, 179.
- (3) Leca-Bouvier, B.; Blum, L. J. *Anal. Lett.* **2005**, *38*, 1491.
- (4) Cooper, M. A. *Anal. Bioanal. Chem.* **2003**, *377*, 834.
- (5) Oh, K. J.; Cash, K. J.; Plaxco, K. W. *Chemistry* **2009**, *15*, 2244.
- (6) Benson, D. E.; Conrad, D. W.; de Lorimer, R. M.; Trammell, S. A.; Hellinga, H. W. *Science* **2001**, *293*, 1641.
- (7) Tyagi, S.; Kramer, F. R. *Nat. Biotechnol.* **1996**, *14*, 303.
- (8) Kohn, J. E.; Plaxco, K. W. *Proc. Natl. Acad. Sci. U.S.A.* **2005**, *102*, 10841.
- (9) Stratton, M. M.; Mitrea, D. M.; Loh, S. N. *ACS Chem. Biol.* **2008**, *3*, 723.
- (10) Plaxco, K. W.; Soh, H. T. *Trends Biotechnol.* **2011**, *29*, 1.
- (11) Vallee-Belisle, A.; Ricci, F.; Plaxco, K. W. *Proc. Natl. Acad. Sci. U.S.A.* **2009**, *106*, 13802.
- (12) Marvin, J. S.; Hellinga, H. W. *Nat. Struct. Biol.* **2001**, *8*, 795.
- (13) Vallee-Belisle, A.; Ricci, F.; Plaxco, K. W. *J. Am. Chem. Soc.* **2011**, *134*, 2876.
- (14) Bryngelson, J. D.; Onuchic, J. N.; Socoli, N. D.; Wolynes, P. G. *Proteins: Struct., Funct. Genet.* **1995**, *21*, 167.
- (15) Garcia-Mira, M. M.; Sadqi, M.; Fischer, N.; Sanchez-Ruiz, J. M.; Muñoz, V. *Science* **2002**, *298*, 2191.
- (16) Yang, W. Y.; Gruebele, M. *Nature* **2003**, *423*, 193.
- (17) Muñoz, V. *Annu. Rev. Biophys. Biomol. Struct.* **2007**, *36*, 395.
- (18) Muñoz, V. *Int. J. Quantum Chem.* **2002**, *90*, 1522.
- (19) Shoemaker, B. A.; Portman, J.; Wolynes, P. G. *Proc. Natl. Acad. Sci. U.S.A.* **2000**, *97*, 8868.
- (20) Naganathan, A. N.; Doshi, U.; Fung, A.; Sadqi, M.; Muñoz, V. *Biochemistry* **2006**, *45*, 8466.
- (21) Li, P.; Oliva, F. Y.; Naganathan, A. N.; Muñoz, V. *Proc. Natl. Acad. Sci. U.S.A.* **2009**, *106*, 103.
- (22) Sadqi, M.; Fushman, D.; Muñoz, V. *Nature* **2006**, *442*, 317.
- (23) Muñoz, V.; Sanchez-Ruiz, J. M. *Proc. Natl. Acad. Sci. U.S.A.* **2004**, *101*, 17646.
- (24) Liu, J.; Campos, L. A.; Cerminara, M.; Wang, X.; Ramanathan, R.; English, D. S.; Muñoz, V. *Proc. Natl. Acad. Sci. U.S.A.* **2012**, *109*, 179.
- (25) Lindorff-Larsen, K.; Piana, S.; Dror, R. O.; Shaw, D. E. *Science* **2011**, *334*, 517.
- (26) Desai, T. M.; Cerminara, M.; Sadqi, M.; Muñoz, V. *J. Biol. Chem.* **2010**, *285*, 34549.
- (27) Oliva, F. Y.; Muñoz, V. *J. Am. Chem. Soc.* **2004**, *126*, 8596.
- (28) Bamford, C. H.; Tipper, C. F. H. *Proton Transfer*; Elsevier: Amsterdam, 1977; Vol. 8.
- (29) Naganathan, A. N.; Doshi, U.; Muñoz, V. *J. Am. Chem. Soc.* **2007**, *129*, 5673.